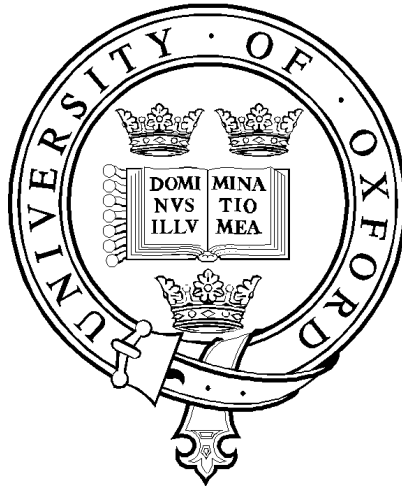


Model Testing of Circular Flat Footings on Uncemented Loose Carbonate Sand: Experimental Data

by

B.W. Byrne and G.T. Houlsby

Report No. OUEL 2192/98



**University of Oxford
Department of Engineering Science
Parks Road, Oxford, OX1 3PJ, U.K.**

**Tel. 01865 273162/283300
Fax. 01865 283301
Email Civil@eng.ox.ac.uk
<http://www-civil.eng.ox.ac.uk/>**

Model Testing of Circular Flat Footings on Uncemented Loose Carbonate Sand: Experimental Data

B.W. Byrne and G.T. Houlsby
The University of Oxford

SUMMARY

This report presents the factual results of a series of combined load tests on a circular flat footing on extremely loose uncemented carbonate sand. These tests were conducted to explore the concepts of work hardening plasticity theory applied to the behaviour of foundations. Similar tests have been completed on clays and dense silica sand. This set of data is to provide empirical evidence of performance on another material. The main intention of the report is to present the results in a systematic manner consistent with previous reports.

INTRODUCTION

Recent studies of footings subjected to combined loads have successfully described the elasto-plastic deformation behaviour of the footing by the use of work hardening plasticity models (Tan, 1990; Martin, 1994; Gottardi *et al.*, 1997). Essentially the postulate is that after a given footing penetration a yield surface is established within $\{V, M/2R, H\}$ space. Any footing behaviour within this surface is assumed to be elastic, whilst elasto-plastic behaviour occurs once the load point reaches the yield surface. This approach can be traced back to Roscoe and Schofield (1956) in their analysis of foundations for steel frames. Butterfield (1980, 1981) developed the idea further and more recent interest has been evident from several research groups world-wide. Primarily this interest has been concentrated on medium to dense silica sands, and clays of increasing strength with depth. This report concentrates on a material with vastly different properties to either of these, and the results serve to illustrate the ease with which the plasticity concept could be adapted to other materials.

EXPERIMENTAL SET-UP

To test the hypothesis it is essential to establish (i) the shape of the yield surface, (ii) the mechanism of hardening of the surface, (iii) a flow rule or plastic potential and (iv) the elastic behaviour within the surface. Studies of this kind normally use eccentric inclined loads (Gottardi *et al.*, 1993), or simply look at the two dimensional cases (V, H) , and, $(V, M/2R)$ (Nova and Montrasio, 1991). At the University of Oxford a loading rig was developed, initially to explore the behaviour of spudcan footings on clay (Martin, 1994). It has undergone several stages of modification and it is adaptable to any soil medium. The unique feature of this apparatus is that any combination of displacement path can be applied to the model footing using computer controlled stepper motors. The response of the footing is determined by measuring the resultant loads using a 'Cambridge' load cell. The displacements are applied using stepper motors, via a stepper motor control unit, with accurate foundation displacements measured using a system of LVDTs. The primary advantage of using this displacement controlled apparatus is the ability to explore post peak behaviour. Primitive load control can also be maintained though the use of feedback on the stepper motors from the load cell, however, the low frequency data logger available during the testing precluded the use of any sophisticated control software. Figure 1 shows the loading rig, further details of which can be gained from Martin (1994) and Gottardi *et al* (1995). Throughout the tests loading rates not exceeding 0.01 mm/s or 0.01 °/s were

used so that any effects of rate became negligible (footing performance was assumed to be rate independent).

The material used for the testing was obtained from a grab sample at the Goodwyn site off the North West Shelf of Western Australia. Carbonate sands can have in-situ void ratios of up to two, and are problematic soils in that upon shearing there can be large volume contraction. For this testing programme the decision was taken to test the material at its loosest state, primarily to maximise the diversity with other data. The material, which had been stored in a saturated state, was firstly dried, then broken up before being sieved to remove the larger shell particles. The sieving process involved two phases, firstly through a 2.36mm sieve to remove any large shell particles, before being passed through a 1mm sieve. Each individual sample was prepared by carefully allowing the material to fall slightly from a scoop into the test container. This method had been used previously in the laboratory for the preparation of uniform loose samples - any slight sample inhomogeneities are averaged out by the large footing displacements that are associated with loose material. A repeatable mean density of 9.32 kN/m³ was obtained. The sample surface was levelled using a vacuum technique, prior to the test sequence. The material possesses a minimum density of 9.22 kN/m³, a maximum density of 11.35 kN/m³, and a grading curve as shown in Figure 2.

RESULTS

A programme of five different test types was undertaken (based on those used by Gottardi *et. al.*, 1995) in order to explore the yield surface shape and the mechanisms associated with yield surface expansion due to hardening. A long capacity displacement transducer system was used, compromising slightly the resolution of the displacement measurements, though entirely necessary due to the quite large displacements that prevailed throughout the testing. This system was used during all tests except for the elasticity tests, where a smaller more accurate measurement system was used to capture the elastic behaviour. The large transducer system necessitates the need to account for the stiffness of the rig between the measured locations and the footing via a 3x3 rig stiffness matrix, [RSM];

$$\begin{Bmatrix} \mathbf{dv} \\ \mathbf{dh} \\ 2R\mathbf{dq} \end{Bmatrix}_{\text{Footing}} = \begin{Bmatrix} \mathbf{dv} \\ \mathbf{dh} \\ 2R\mathbf{dq} \end{Bmatrix}_{\text{Measured}} + [RSM] \begin{Bmatrix} V \\ H \\ M / 2R \end{Bmatrix}$$

where [RSM] is defined as;

$$\begin{bmatrix} -5.09\text{E} - 04 & -1.07\text{E} - 04 & 8.92\text{E} - 06 \\ 1.72\text{E} - 06 & -2.06\text{E} - 03 & 2.49\text{E} - 04 \\ 8.31\text{E} - 04 & 3.83\text{E} - 03 & -1.81\text{E} - 03 \end{bmatrix} \text{ for } H > 0 \text{ and } \begin{bmatrix} -5.09\text{E} - 04 & -1.07\text{E} - 04 & 8.92\text{E} - 06 \\ -1.60\text{E} - 04 & -2.06\text{E} - 03 & 2.61\text{E} - 04 \\ 8.31\text{E} - 04 & 3.83\text{E} - 03 & -1.81\text{E} - 03 \end{bmatrix} \text{ for } H < 0,$$

where the displacements are in mm and forces in N.

From a plasticity point of view the use of the large LVDTs was justified as the vertical soil stiffness ratios, v_{ke}/v_{kp} , were typically greater than 50, which suggested that any load path tracked during the constant penetration tests would in fact closely approximate a yield surface. The effect of rig stiffness on the shape of this tracked yield surface could also be assumed to be negligible. A footing of diameter 150mm, and side-wall of 70mm, was used which, when loaded to 1600N, displaced to a vertical penetration of about 60mm - an indication of the compressibility of the soil.

Table 1 displays the 18 tests completed (grouping them within specific test types), whilst Table 2 gives a complete listing of all the available data files corresponding to each test.

The data files contain fully processed data including the incorporation of the effect of rig stiffness on footing displacements, as well as correction of the vertical and horizontal load for rotation of the footing. The data in each file are ordered as (note that the moment loads and rotational displacements are normalised by $2R$):

Column 1	Column 2	Column 3	Column 4	Column 5	Column 6	Column 7
Time	Vertical Load	Horizontal Load	Moment Load	Vertical Displacement	Horizontal Displacement	Rotational Displacement
t	V	H	$M/2R$	dw	du	$2Rdq$
Seconds	Newtons	Newtons	Newtons	millimetres	millimetres	millimetres

The co-ordinate systems, sign conventions and notations for the loads and displacements are shown in Figure 3 following that set out by Butterfield *et. al.* (1997). The load reference point was located at the centre of the base of the footing (*ie* mudline) as defined in Figure 3, consistent with previous work conducted on flat footings at Oxford University.

The data are presented graphically in this report in two forms. Figure 4 through to Figure 21 depicts the time histories of the various tests. Figure 22 through to Figure 69 depicts the stress/strain relationships, load paths, and displacement paths followed during the specific events of each test.

CONCLUSIONS

This report has presented the results from 18 general loading tests on a circular footing on a loose uncemented carbonate sand. The tests were specifically completed to complement tests performed on dense silica sand in order to provide proof of the versatility of a plasticity formulation of response. Whilst specific interpretation of the results have not been carried out in this report it is clear that enough information will be available to determine parameters for a suitable plasticity model.

ACKNOWLEDGEMENTS

The first author would like to gratefully acknowledge the generous support of the Rhodes Trust. This work could not have been completed if it were not for Phillip Watson and Gerard Dyson of the University of Western Australia who, whilst visiting the Civil Engineering group at Oxford, helped with carrying out the testing and preparatory work.

REFERENCES

- Butterfield, R. 1980. A simple analysis of the load capacity of rigid footings on granular materials. *Journee de Geotechnique*, ENTPE, Lyon, France, pp 128-137
- Butterfield, R. 1981. Another look at gravity platform foundations. *SMFE in Offshore Technology*, CISM, Udine, Italy.
- Butterfield, R., Housby, G.T. and Gottardi, G. 1997. Standardised sign conventions and notation for generally loaded foundations. *Geotechnique*, Vol 47, N^o 4, UK.
- Gottardi, G. and Butterfield, R. 1993. On the bearing capacity of circular footings on sand under eccentric and inclined loads. *Soils and Foundations* **33**, N^o 3, pp 68-79.
- Gottardi, G. and Housby, G.T. 1995. Model tests of circular footings on sand subjected to combined loads. *Report N^o OUEL 2071/95*. Oxford University Engineering Laboratory, UK.
- Gottardi, G., Housby, G.T. and Butterfield, R. 1997. The plastic response of circular footings on sand under general planar loading. *Report N^o OUEL 2143/97*. Oxford University Engineering Laboratory, UK.

- Martin, C.M. 1994. *Physical and numerical modelling of offshore foundations under combined loads*. DPhil Thesis, University of Oxford, UK.
- Nova, R and Montrasio, L. 1991. Settlements of shallow foundations on sand. *Geotechnique* **41**, N° 2, pp 243-256.
- Roscoe, K.H. and Schofield, A.N. 1956. The stability of short pier foundations on sand, discussion. *British Welding Journal*, January, pp 12-18.
- Tan, F.S.C. 1990. *Centrifuge and numerical modelling of conical footings on sand*. PhD Thesis, University of Cambridge, UK.

Test Group	Test Notes	Test Names	Notes
Vertical Loading	As far as possible with unload-reload cycles	FUF01, FUF02	
	Up to V = 1600N, with unload-reload cycles at V = 1000N	FUF05, FUF06, FUF08, FUF09, FUF10, FUF11, FUF13, FUF14, FUF15, FUF16, FUF23	
Swipe	From V = 1600N	FUF05 (H, 0)	$\text{atan}(2R\delta\theta/\delta u) = 0.03$
		FUF06 (0, M)	$\text{atan}(2R\delta\theta/\delta u) = 89.6$
		FUF08 (H, M)	$\text{atan}(2R\delta\theta/\delta u) = 69.1$
		FUF09 (H, -M)	$\text{atan}(2R\delta\theta/\delta u) = -69.4$
	From V = 50N after V = 1600N	FUF10 (H, 0)	$\text{atan}(2R\delta\theta/\delta u) = -0.4$
		FUF11 (0, M)	$\text{atan}(2R\delta\theta/\delta u) = 89.7$
Multiple values of V	FUF21 (H, 0) from V = 400N, 800N, 1200N, 1600N and 1800N	$\text{atan}(2R\delta\theta/\delta u) = 2.2$ $\text{atan}(2R\delta\theta/\delta u) = 2.5$ $\text{atan}(2R\delta\theta/\delta u) = 0.8$ $\text{atan}(2R\delta\theta/\delta u) = 2.9$ $\text{atan}(2R\delta\theta/\delta u) = 0.9$	
Constant V	At V = 1600N	FUF13 (H, 0)	$\text{atan}(2R\delta\theta/\delta u) = 1.2$
		FUF14 (0, M)	$\text{atan}(2R\delta\theta/\delta u) = 87.9$
		FUF15 (H, M)	$\text{atan}(2R\delta\theta/\delta u) = 68.7$
		FUF16 (H, -M)	$\text{atan}(2R\delta\theta/\delta u) = -72.9$
Monotonic Radial Displacement	Each test taken as far as possible	FUF17	$\delta u/\delta w = 0.997$
		FUF18	$\delta u/\delta w = 1.509$
		FUF19	$2R\delta\theta/\delta w = 0.491$
		FUF20	$2R\delta\theta/\delta w = 2.356$
Elastic Cycles	At V = 800N after V = 1600N	FUF23	V ± 100N excursion H ± 100N excursion M/2R ± 50N excursion

Table 2 - Summary of the tests undertaken during study.

Test	Density (kN/m ³)	Description	Datafiles			Velocity Data (Actual velocities and distances)
			Name	Description	Lines	
FUF01	9.389	Vertical loading test Unload-reload at V=500N Unload-reload at V=1000N Unload-reload at V=1600N	fuf01_1.dat fuf01_2.dat fuf01_3.dat fuf01.ps (4) ¹ fuf01.dat fuf01e.ps (22, 23)	} } All data logged during test } Total test postscript file Vertical load data file Vertical load postscript file	822 653 2528 - 4003 -	v _d = 0.01 mm/s v _u = 0.005 mm/s
FUF02	9.235	Vertical loading test Unload-reload at V=500N Unload-reload at V=1000N Unload-reload at V=1600N	fuf02_1.dat fuf02.ps (5) fuf02.dat fuf02e.ps (24, 25)	All data logged during test Total test postscript file Vertical load data file Vertical load postscript file	1979 - 1979 -	v _d = 0.01 mm/s v _u = 0.005 mm/s
FUF05	9.245	(H,0) swipe at V=1600N Unload-reload at V=1000N	fuf05_1.dat fuf05_2.dat fuf05_3.dat fuf05.ps (6) fuf05.dat fuf05e.ps (26, 27)	} } All data logged during test } Total test postscript file Datafile for swipe from V=1600N Postscript file for swipe from V=1600N	964 896 1541 - 1398 -	v _d = 0.01 mm/s v _u = 0.005 mm/s v _h = 0.0097 mm/s (15.12 mm)
FUF06	9.237	(0,M) swipe at V=1600N Unload-reload at V=1000N	fuf06_1.dat fuf06_2.dat fuf06_3.dat fuf06.ps (7) fuf06.dat fuf06e.ps (28, 29)	} } All data logged during test } Total test postscript file Datafile for swipe from V=1600N Postscript file for swipe from V=1600N	924 653 998 - 844 -	v _d = 0.01 mm/s v _u = 0.005 mm/s v _{2R0} = 0.025 mm/s (27.99 mm)
FUF08	9.452	(H,M) swipe at V=1600N Unload-reload at V=1000N	fuf08_1.dat fuf08_2.dat fuf08_3.dat fuf08_4.dat fuf08.ps (8) fuf08.dat fuf08e.ps (30, 31)	} } All data logged during test } } Total test postscript file Datafile for swipe from V=1600N Postscript file for swipe from V=1600N	20 888 678 880 - 726 -	v _d = 0.01 mm/s v _u = 0.005 mm/s v _h = 0.0097 mm/s (7.85 mm) v _{2R0} = 0.026 mm/s (20.56 mm)

¹ Numbers in brackets correspond to the figure number in this report.

Test	Density (kN/m ³)	Description	Datafiles			Velocity Data (Actual velocities and distances)
			Name	Description	Lines	
FUF09	9.402	(H,-M) swipe at V=1600N Unload-reload at V=1000N	fuf09_1.dat fuf09_2.dat fuf09.ps (9) fuf09.dat fuf09e.ps (32, 33)	} All data logged during test } Total test postscript file Datafile for swipe from V=1600N Postscript file for swipe from V=1600N	1202 876 - 724 -	v _d = 0.01 mm/s v _u = 0.005 mm/s v _h = 0.0096 mm/s (7.72 mm) v _{2R0} = 0.025 mm/s (-20.52 mm)
FUF10	9.288	(H,0) swipe at V=50N after V=1600N Unload-reload at V=1000N	fuf10_1.dat fuf10_2.dat fuf10_3.dat fuf10_4.dat fuf10_5.dat fuf10.ps (10) fuf10.dat fuf10e.ps (34, 35)	} } } All data logged during test } } Total test postscript file Datafile for swipe from V=50N Postscript file for swipe from V=50N	436 566 14 347 1555 - 922 -	v _d = 0.01 mm/s v _u = 0.005 mm/s v _h = 0.0096 mm/s (9.78 mm)
FUF11	9.339	(0,M) swipe at V=50N after V=1600N Unload-reload at V=1000N	fuf11_1.dat fuf11_2.dat fuf11_3.dat fuf11.ps (11) fuf11.dat fuf11e.ps (36, 37)	} } All data logged during test } Total test postscript file Datafile for swipe from V=50N Postscript file for swipe from V=50N	1055 288 1474 - 773 -	v _d = 0.01 mm/s v _u = 0.005 mm/s v _{2R0} = 0.025 mm/s (25.56 mm)
FUF13	9.388	(H,0) at constant V=1600N Unload-reload at V=1000N	fuf13_1.dat fuf13_2.dat fuf13.ps (12) fuf13.dat fuf13e.ps (38, 39)	} All data logged during test } Total test postscript file Datafile for swipe at V=1600N Postscript file for swipe at V=1600N	1675 1046 - 773 -	v _d = 0.01 mm/s v _u = 0.005 mm/s v _h = 0.0089 mm/s (9.07 mm)
FUF14	9.334	(0,M) at constant V=1600N Unload-reload at V=1000N	fuf14_1.dat fuf14_2.dat fuf14.ps (13) fuf14.dat fuf14e.ps (40, 41)	} All data logged during test } Total test postscript file Datafile for swipe at V=1600N Postscript file for swipe at V=1600N	1282 964 - 498 -	v _d = 0.01 mm/s v _u = 0.005 mm/s v _{2R0} = 0.025 mm/s (14.19 mm)

Test	Density (kN/m ³)	Description	Datafiles			Velocity Data (Actual velocities and distances)
			Name	Description	Lines	
FUF15	9.245	(H,M) at constant V=1600N Unload-reload at V=1000N	fuf15_1.dat fuf15_2.dat fuf15_3.dat fuf15.ps (14) fuf15.dat fuf15e.ps (42, 43)	} } All data logged during test } Total test postscript file Datafile for swipe at V=1600N Postscript file for swipe at V=1600N	536 1194 647 - 461 -	v _d = 0.01 mm/s v _u = 0.005 mm/s v _h = 0.0094 mm/s (4.94 mm) v _{2R0} = 0.024 mm/s (12.68 mm)
FUF16	9.422	(H,-M) swipe at constant V=1600N Unload-reload at V=1000N	fuf16_1.dat fuf16_2.dat fuf16.ps (15) fuf16.dat fuf16e.ps (44, 45)	} All data logged during test } Total test postscript file Datafile for swipe at V=1600N Postscript file for swipe at V=1600N	1561 675 - 444 -	v _d = 0.01 mm/s v _u = 0.005 mm/s v _h = 0.0076 mm/s (3.86 mm) v _{2R0} = 0.025 mm/s (-12.61 mm)
FUF17	9.260	Monotonic radial displacement Du/dw = 1	fuf17_1.dat fuf17_2.dat fuf17_3.dat fuf17.ps (16) fuf17.dat fuf17e.ps (46, 47)	} } All data logged during test } Total test postscript file Datafile for radial displacement Postscript file for radial displacement	5 50 1011 - 1061 -	v _d = 0.0091 mm/s (41.06 mm) v _h = 0.0091 mm/s (40.97 mm)
FUF18	9.502	Monotonic radial displacement Du/dw = 1.5	fuf18_1.dat fuf18.ps (17) fuf18.dat fuf18e.ps (48, 49)	All data logged during test Total test postscript file Datafile for radial displacement Postscript file for radial displacement	1233 - 1184 -	v _d = 0.0062 mm/s (31.08 mm) v _h = 0.0094 mm/s (46.91 mm)
FUF19	9.427	Monotonic radial displacement 2rdq/dw = 0.5	fuf19_1.dat fuf19.ps (18) fuf19.dat fuf19e.ps (50, 51)	All data logged during test Total test postscript file Datafile for radial displacement Postscript file for radial displacement	1457 - 1184 -	v _d = 0.0094 mm/s (46.97 mm) v _{2R0} = 0.0046 mm/s (23.08 mm)
FUF20	9.381	Monotonic radial displacement 2Rdq/dw = 2.35	fuf20_1.dat fuf20.ps (19) fuf20.dat fuf20e.ps (52, 53)	All data logged during test Total test postscript file Datafile for radial displacement Postscript file for radial displacement	568 - 568 -	v _d = 0.0073 mm/s (11.77 mm) v _{2R0} = 0.017 mm/s (27.73 mm)

Test	Density (kN/m ³)	Description	Datafiles			Velocity Data (Actual velocities and distances)
			Name	Description	Lines	
FUF21	9.407	(H,0) multiple swipes at V=400N, 800N, 1200N, 1600N and 1800N	fuf21_1f.dat fuf21_2f.dat fuf21_3f.dat fuf21_4f.dat fuf21_5f.dat fuf21_6f.dat fuf21.ps (20) fuf21_1.dat fuf21_2.dat fuf21_3.dat fuf21_4.dat fuf21_5.dat fuf21_1.ps (54, 55) fuf21_2.ps (56, 57) fuf21_3.ps (58, 59) fuf21_4.ps (60, 61) fuf21_5.ps (62, 63) fuf21all.ps (64, 65)	} } } All data logged during test } } } } Total test postscript file Datafile for swipe from V=400N Datafile for swipe from V=800N Datafile for swipe from V=1200N Datafile for swipe from V=1600N Datafile for swipe from V=1800N Postscript file for swipe from V=400N Postscript file for swipe from V=800N Postscript file for swipe from V=1200N Postscript file for swipe from V=1600N Postscript file for swipe from V=1800N Postscript file for all swipe events	242 259 2541 14 829 523 - 225 223 271 358 352 - - - - - -	v _d = 0.01 mm/s v _h = 0.009 mm/s (2.27 mm) v _h = 0.0088 mm/s (2.22 mm) v _h = 0.0084 mm/s (2.56 mm) v _h = 0.0087 mm/s (3.48 mm) v _h = 0.0082 mm/s (3.24 mm)
FUF23	9.342	Elastic cycles at V=800N after V=1600N Unload-reload at V=1000N 2 sets of cycles about V=800N	fuf23_1f.dat fuf23_2f.dat fuf23_3f.dat fuf23_4f.dat fuf23_5f.dat fuf23.ps (21) fuf23_1.dat fuf23_2.dat fuf23_1.ps (66, 67) fuf23_2.ps (68, 69)	} } All data logged during test } } } } Total test postscript file Datafile for first set of cycles Datafile for second set of cycles Postscript file for first set of cycles Postscript file for second set of cycles	767 1570 1495 1621 9 - 1311 1289 - -	v _d = 0.01 mm/s v _u = 0.005 mm/s Elasticity Cycles v _v = 0.0008 mm/s (± 100 N) v _h = 0.00032 mm/s (± 100 N) v _{2R0} = 0.0027 mm/s (± 54 N)

Table 3 - Summary of data files associated with the testing.



Figure 1 - Photograph of the three degree of freedom loading rig located at The University of Oxford.

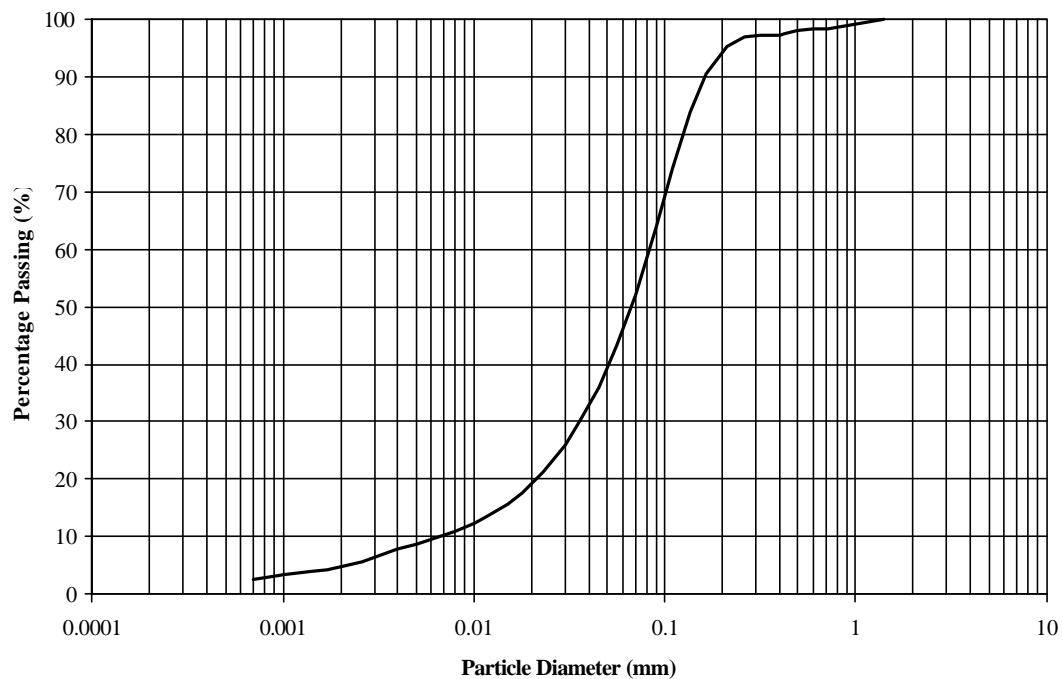


Figure 2 - Grading curve for the Goodwyn Carbonate sand utilised during the experiments

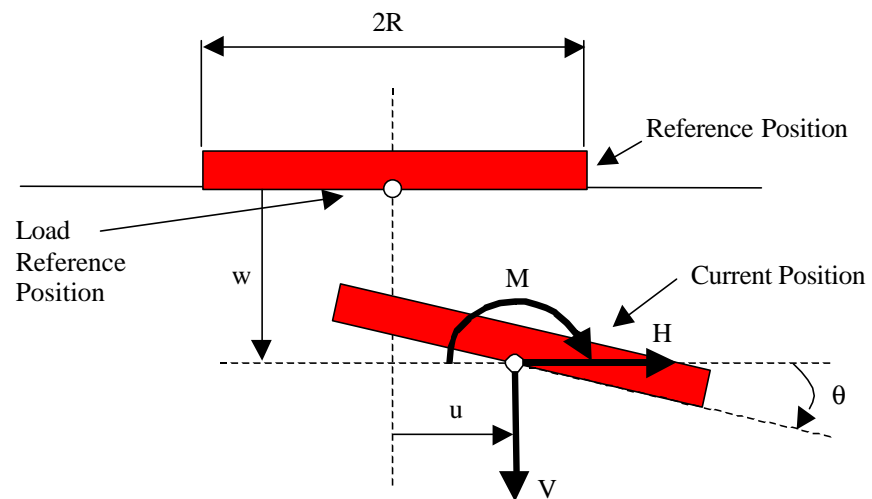
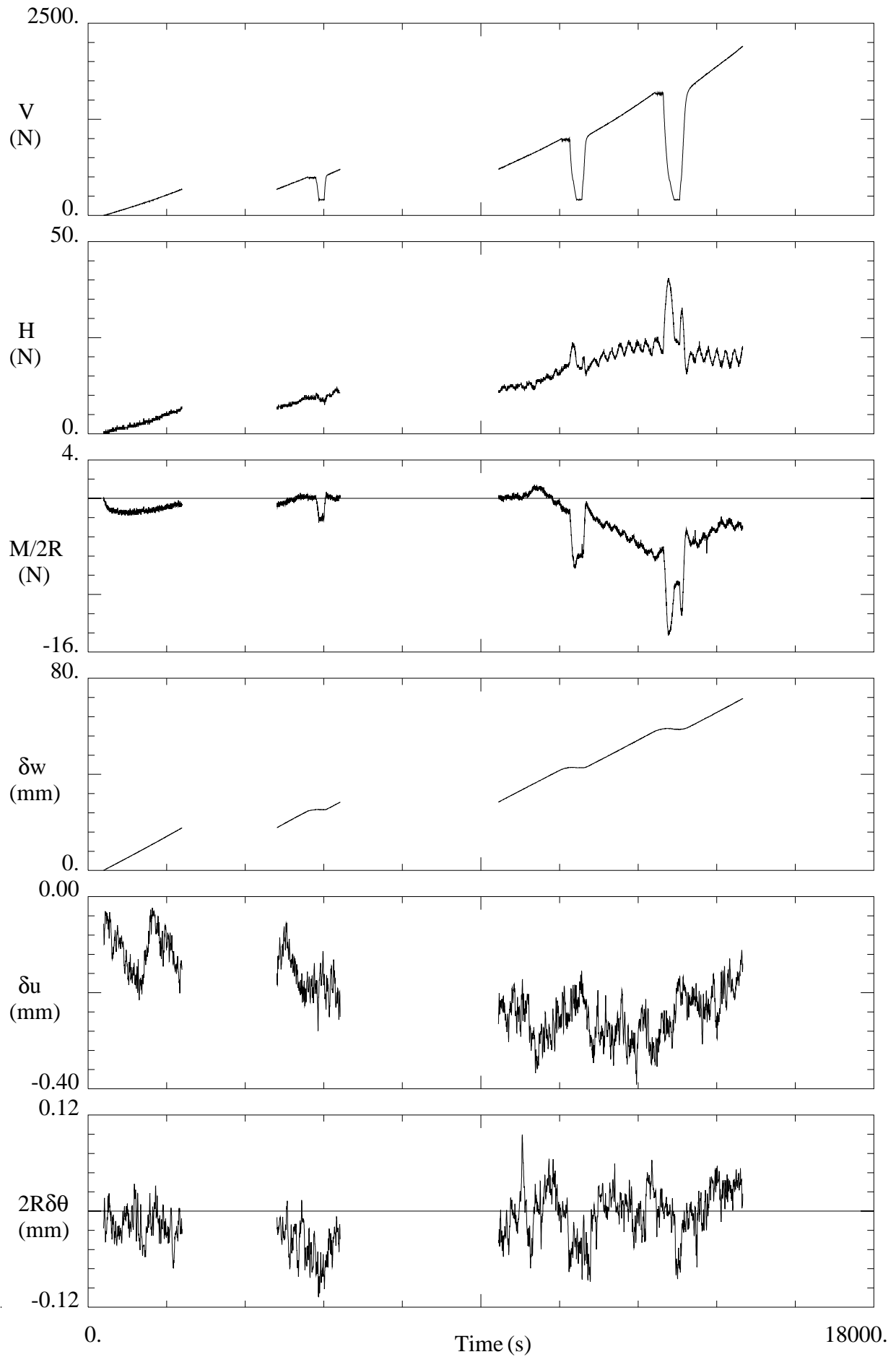
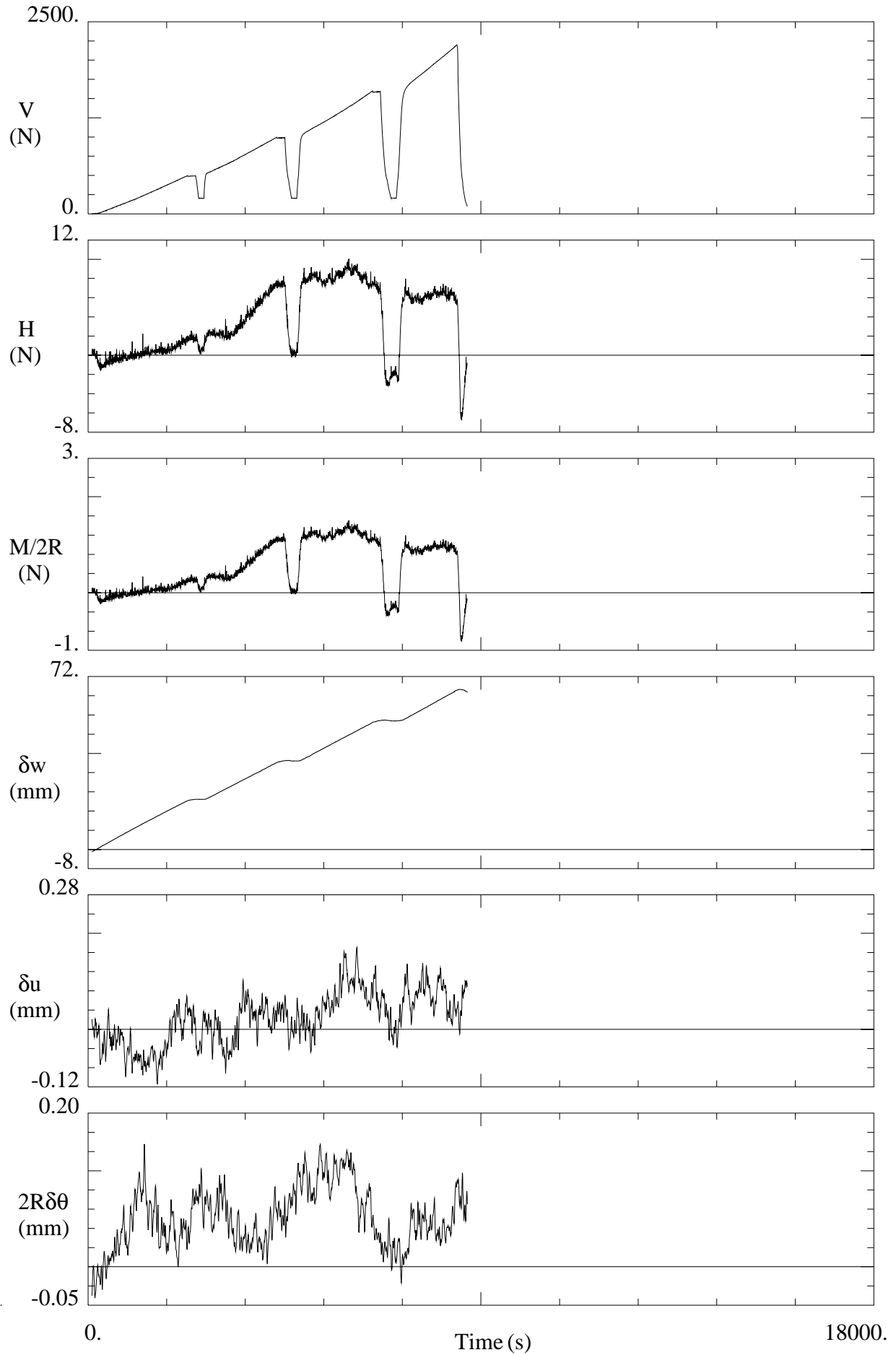


Figure 3 - Sign convention and notation (after Butterfield *et al*, 1997)

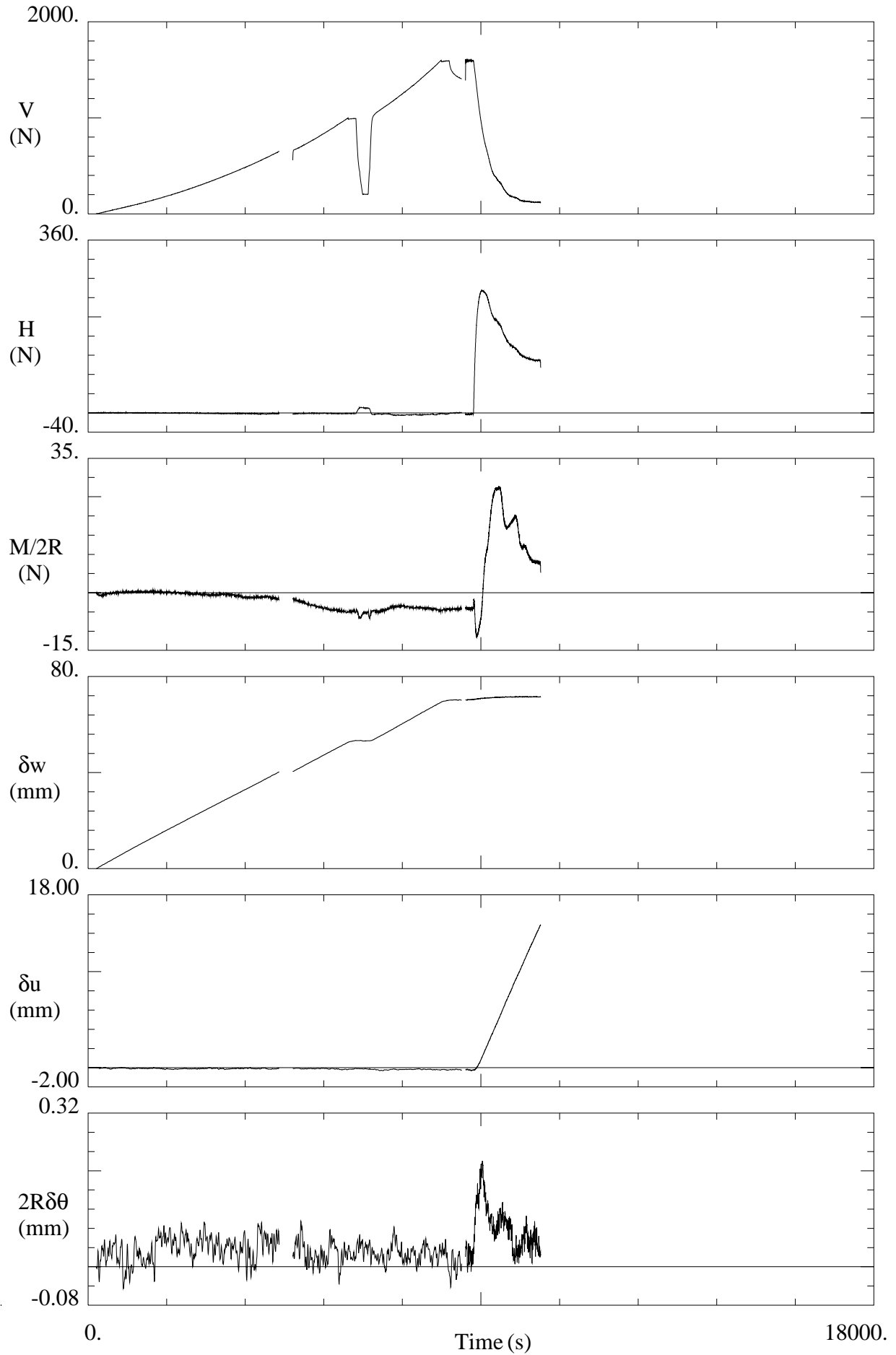
Oxford University: Carbonate Sand Footing Tests
Test FUF01: Vertical Loading Test

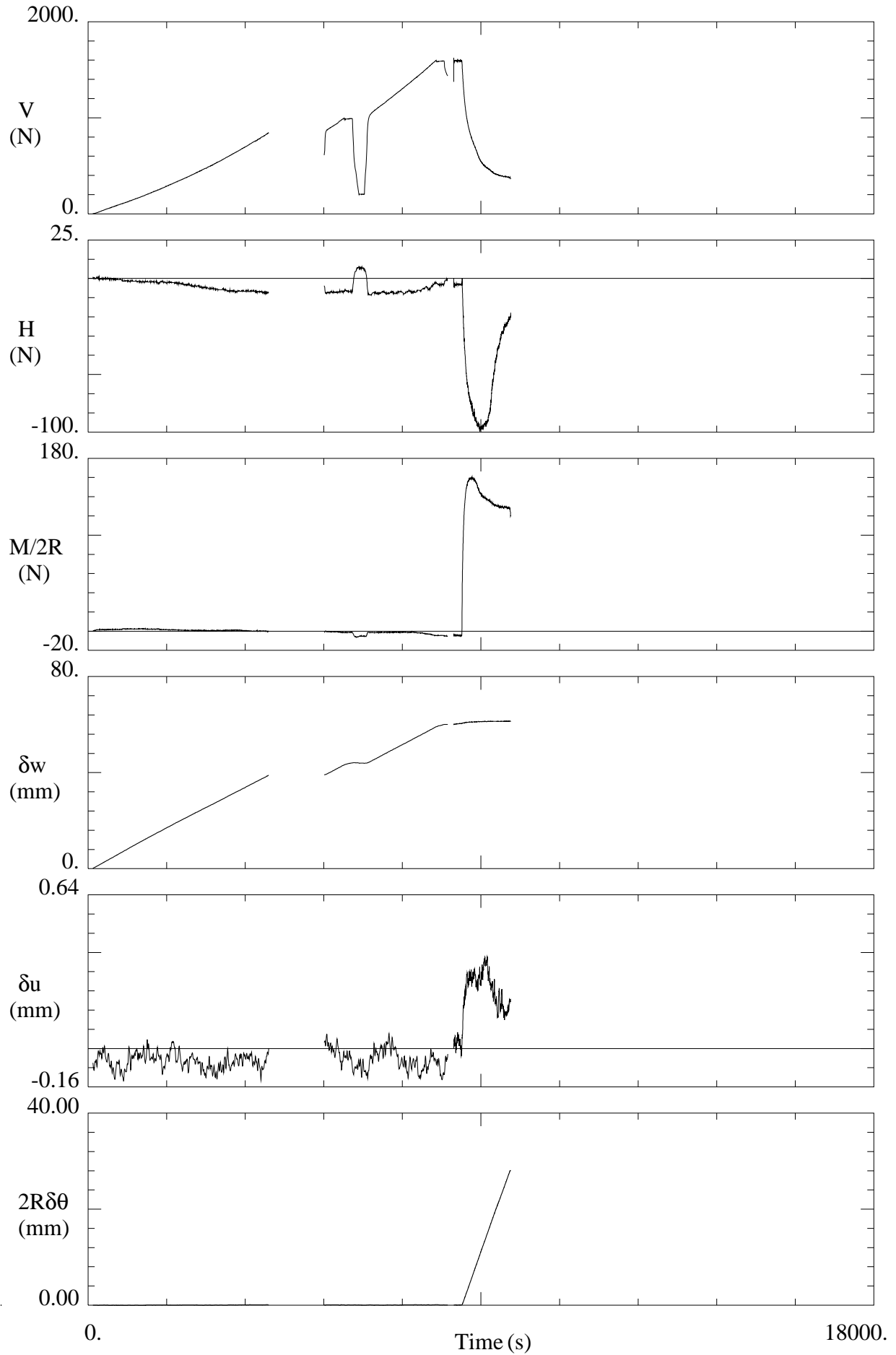


Oxford University: Carbonate Sand Footing Tests
Test FUF02: Vertical Loading Test

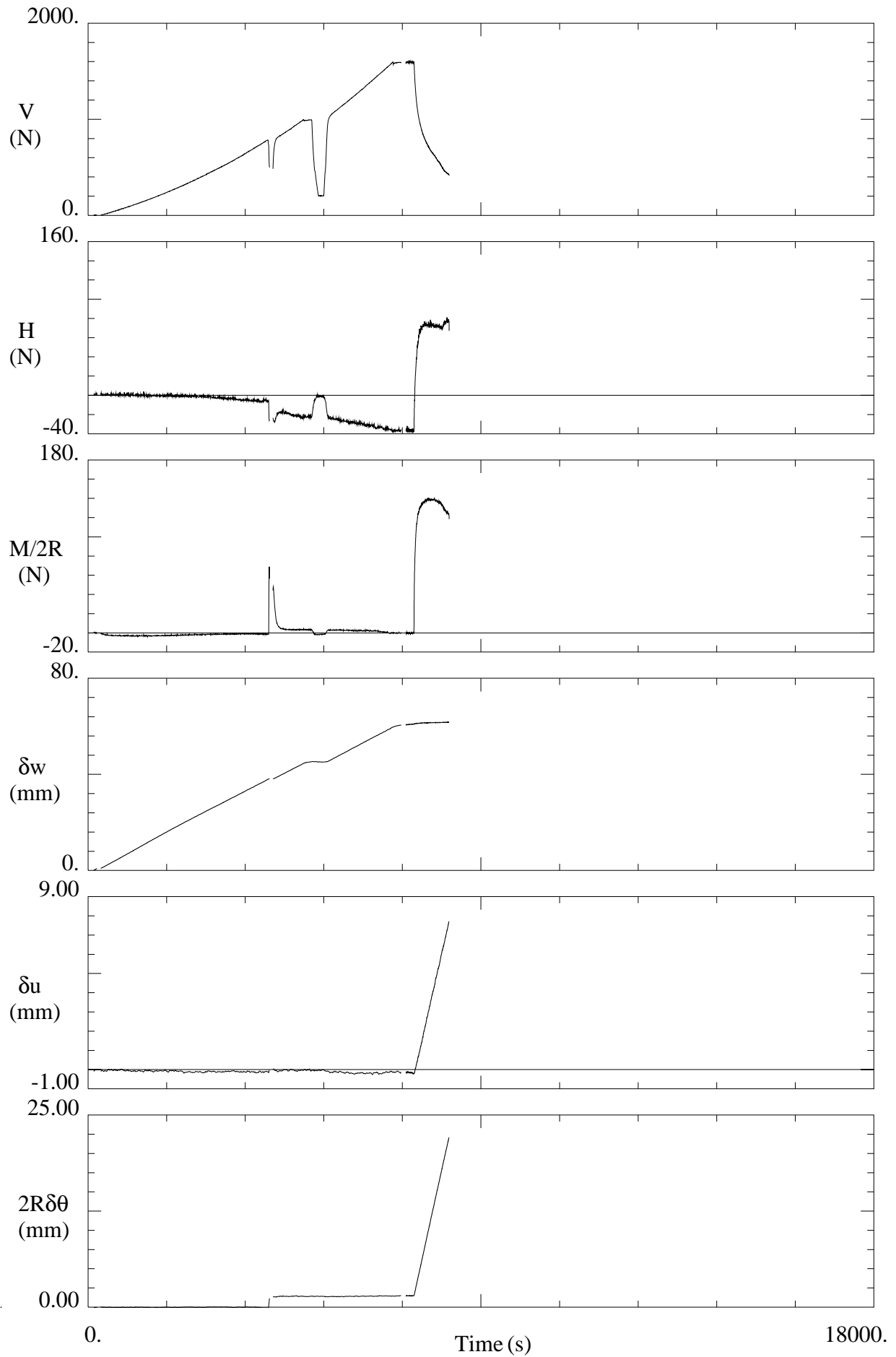


Oxford University: Carbonate Sand Footing Tests
Test FUF05: (H,0) Swipe from V=1600N

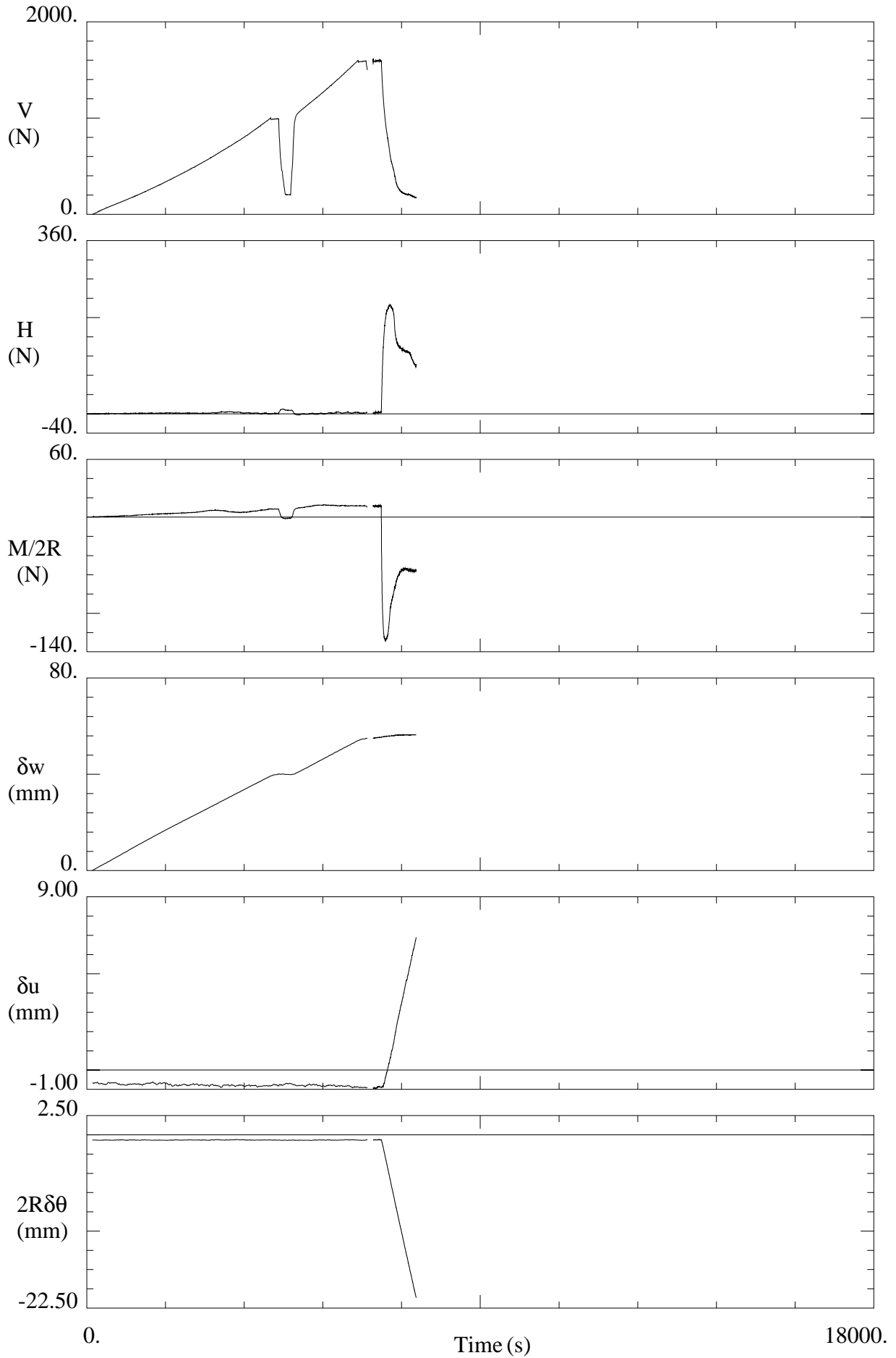


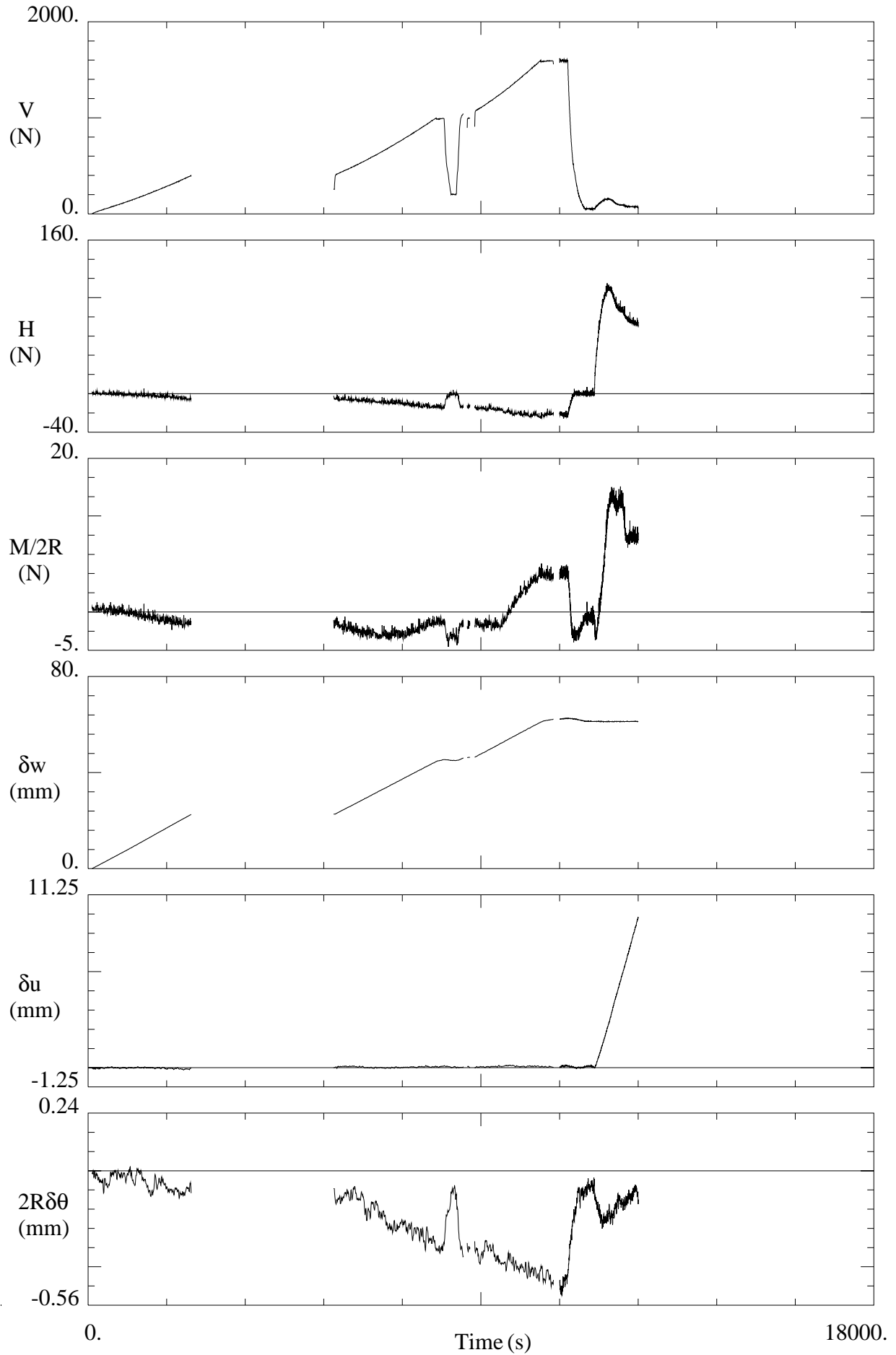


Oxford University: Carbonate Sand Footing Tests
Test FUF08: (H,M) Swipe from V=1600N

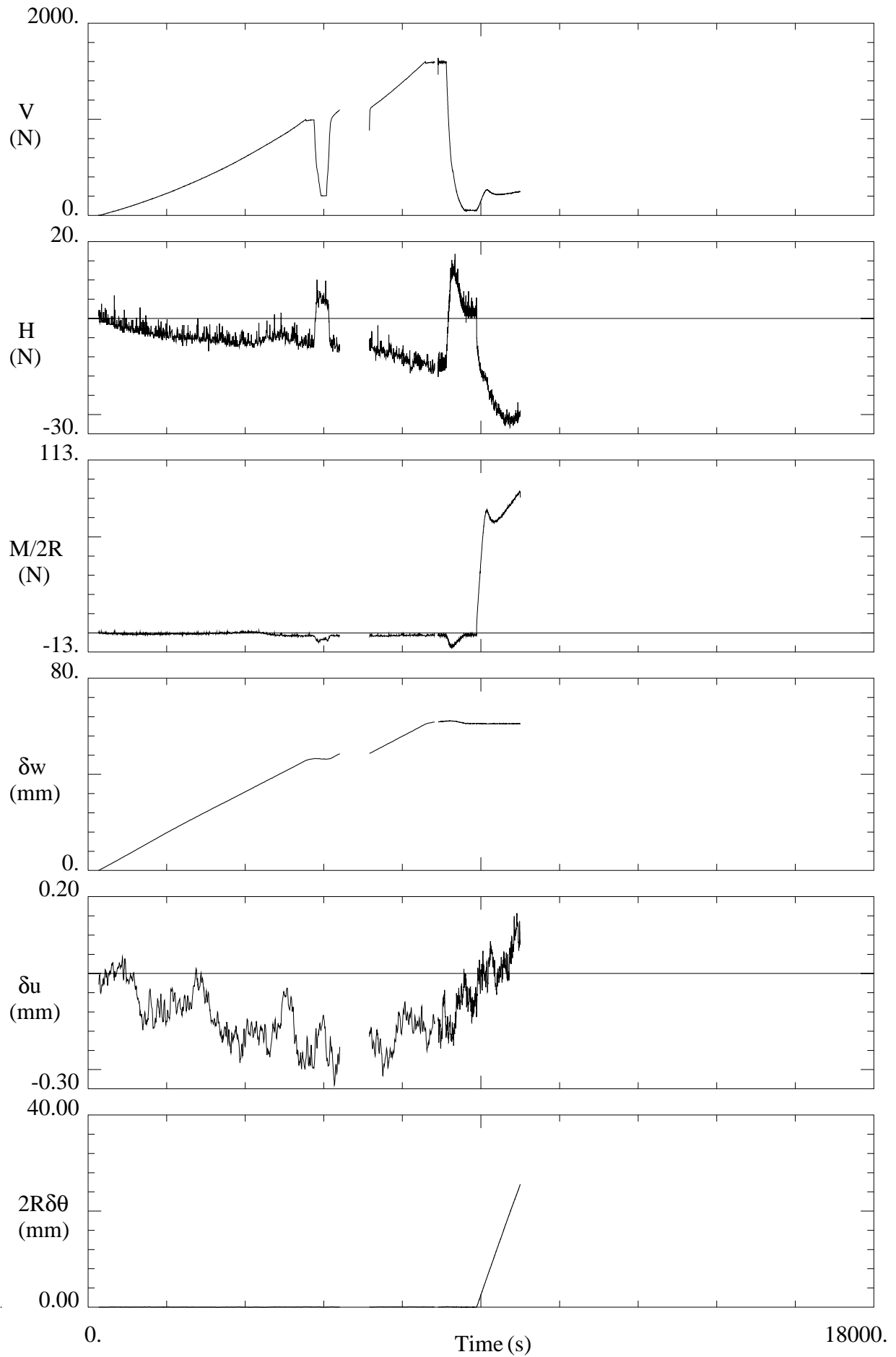


Oxford University: Carbonate Sand Footing Tests
Test FUF09: (H,-M) Swipe from V=1600N

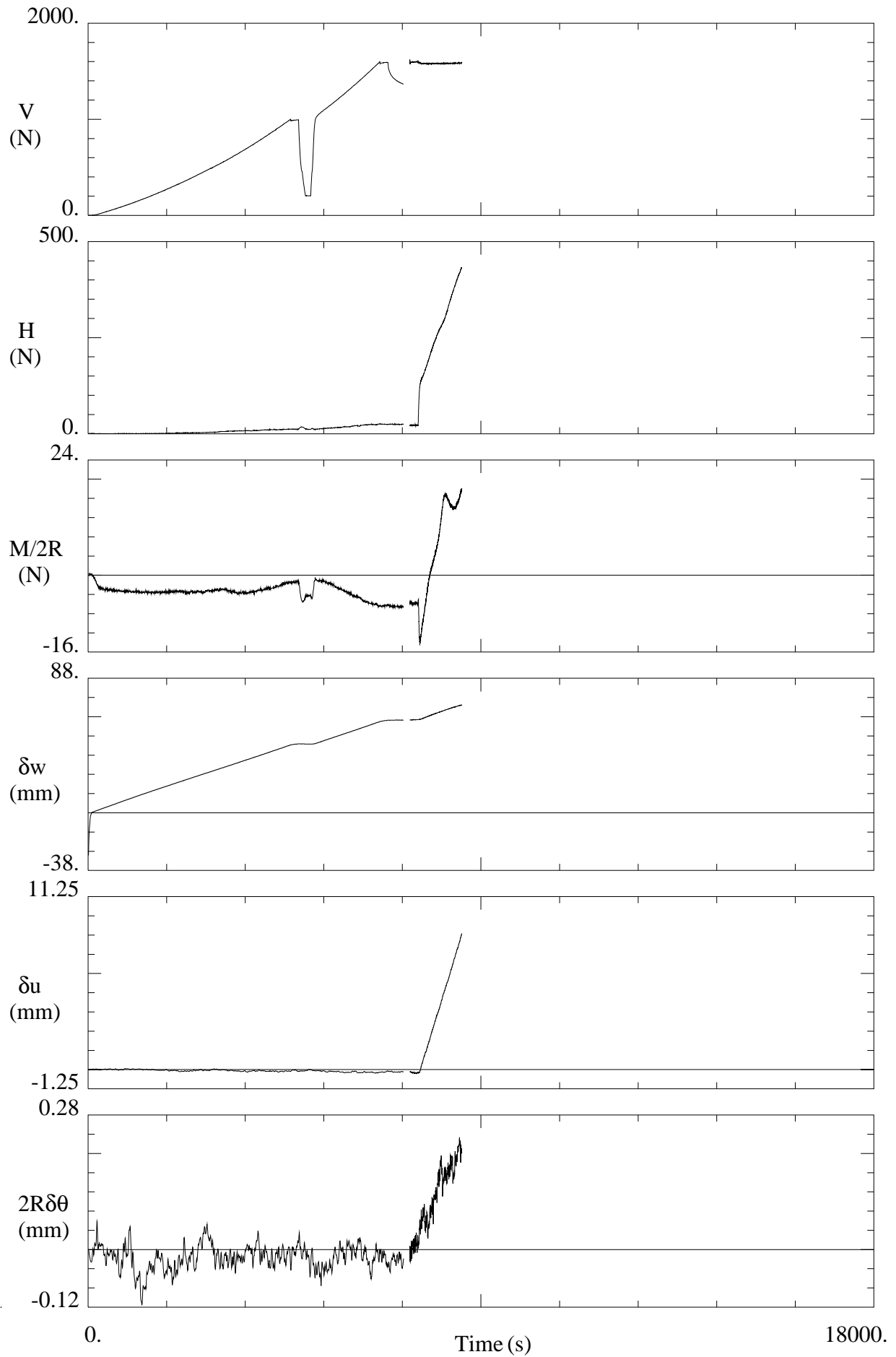




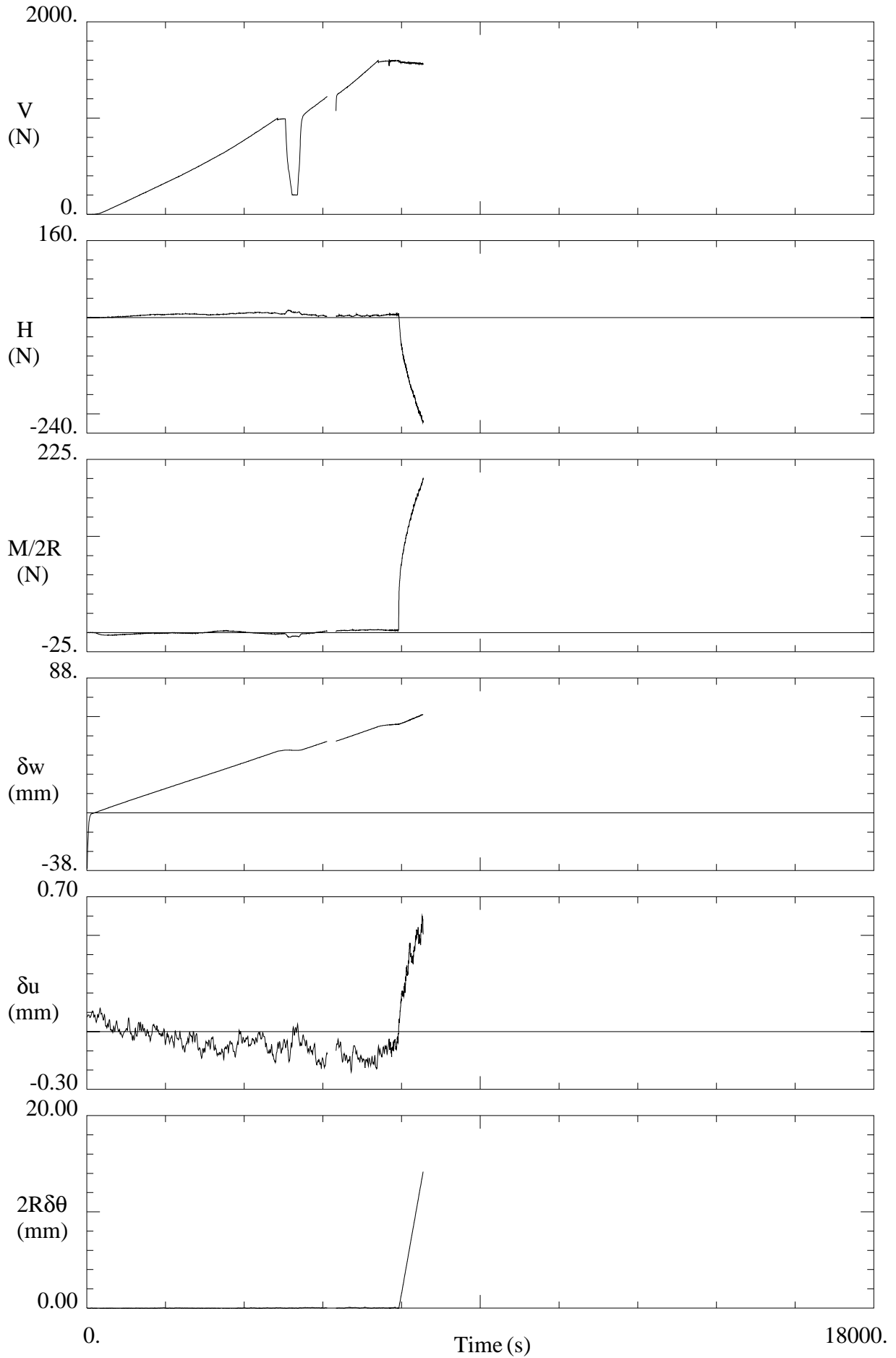
Oxford University: Carbonate Sand Footing Tests
Test FUF11: (0,M) Swipe from V=50N after V=1600N

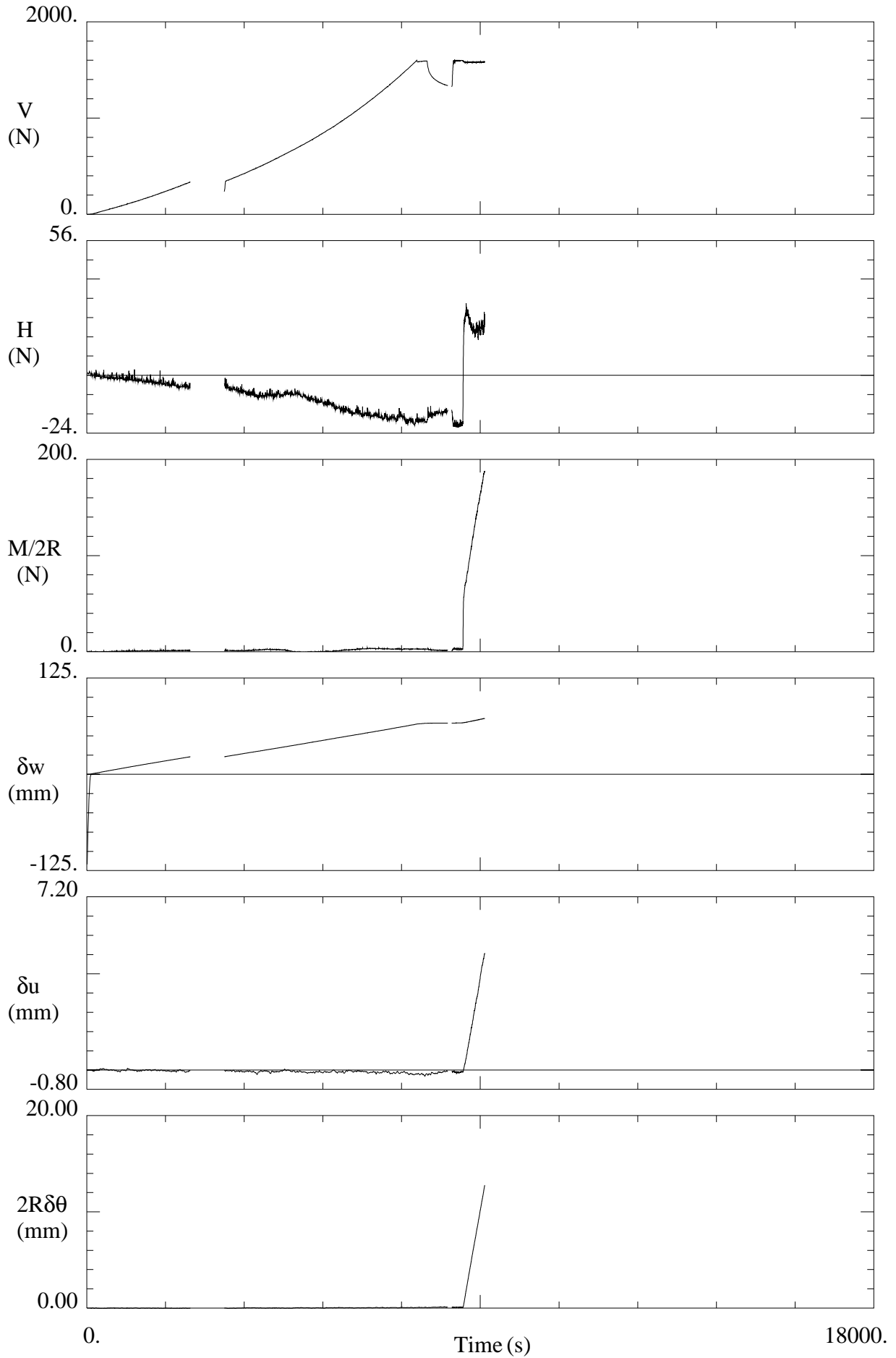


Oxford University: Carbonate Sand Footing Tests
Test FUF13: (H,0) Swipe at Constant V=1600N

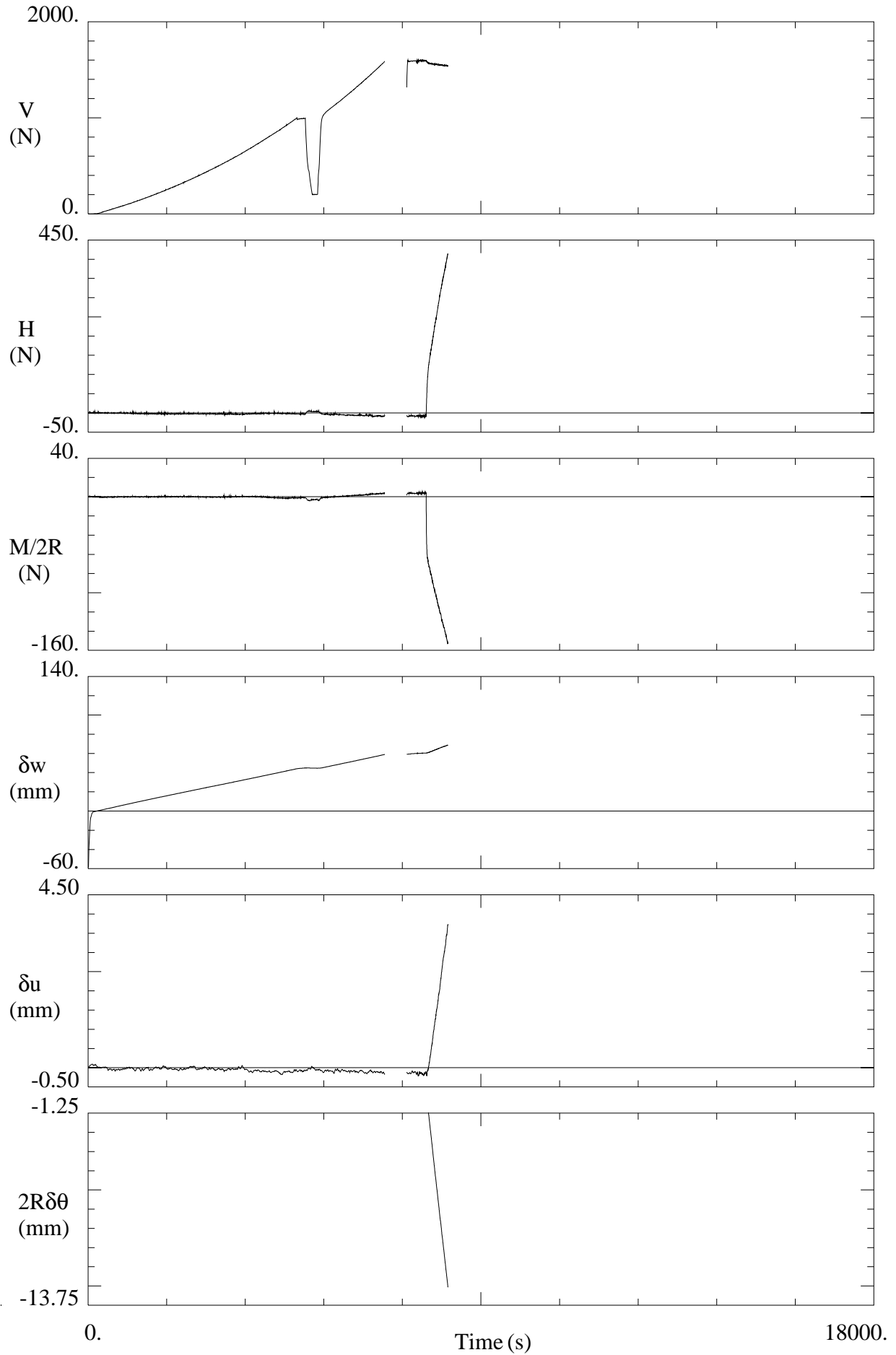


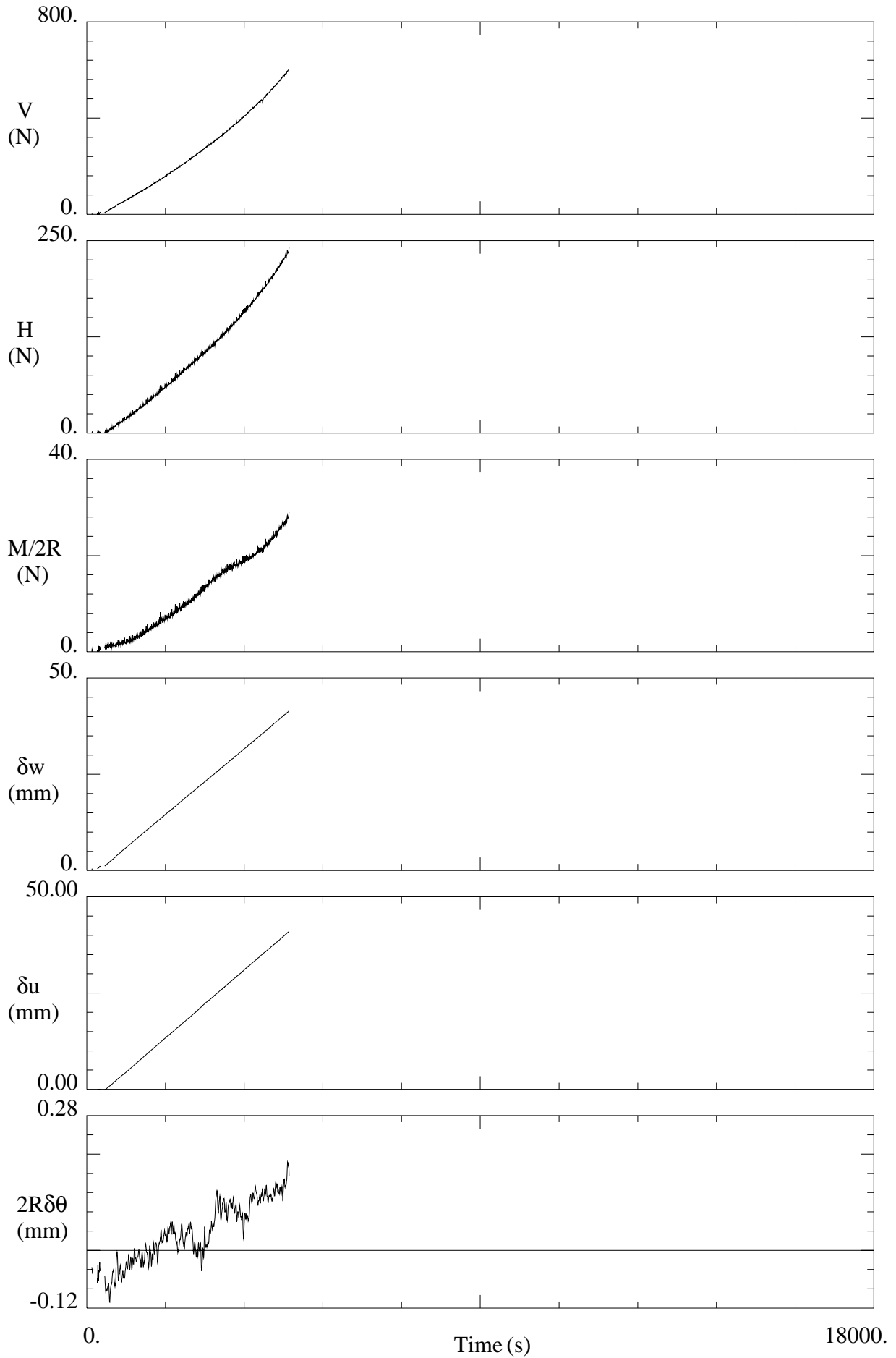
Oxford University: Carbonate Sand Footing Tests
Test FUF14: (0,M) Swipe at Constant V=1600N

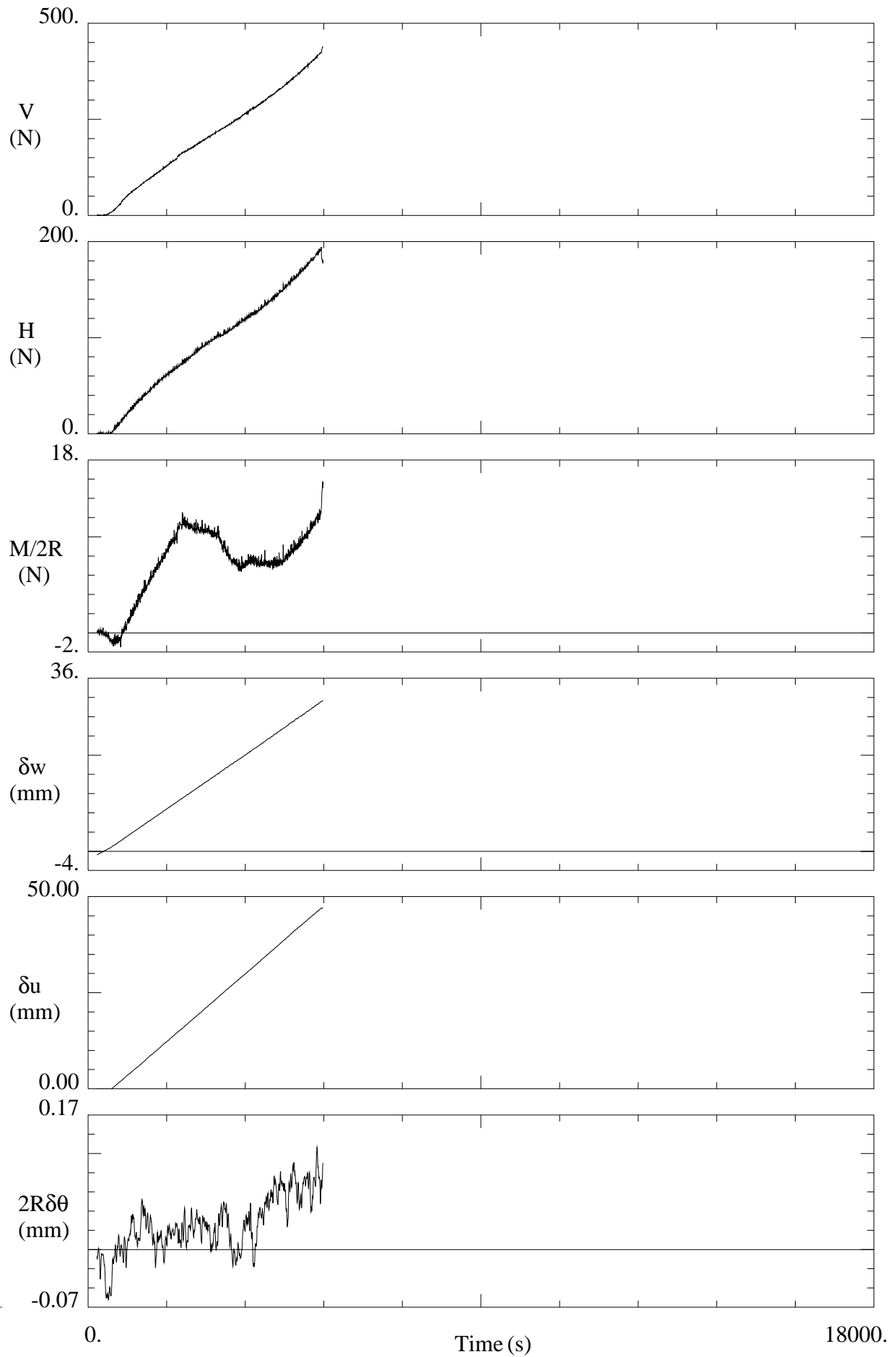


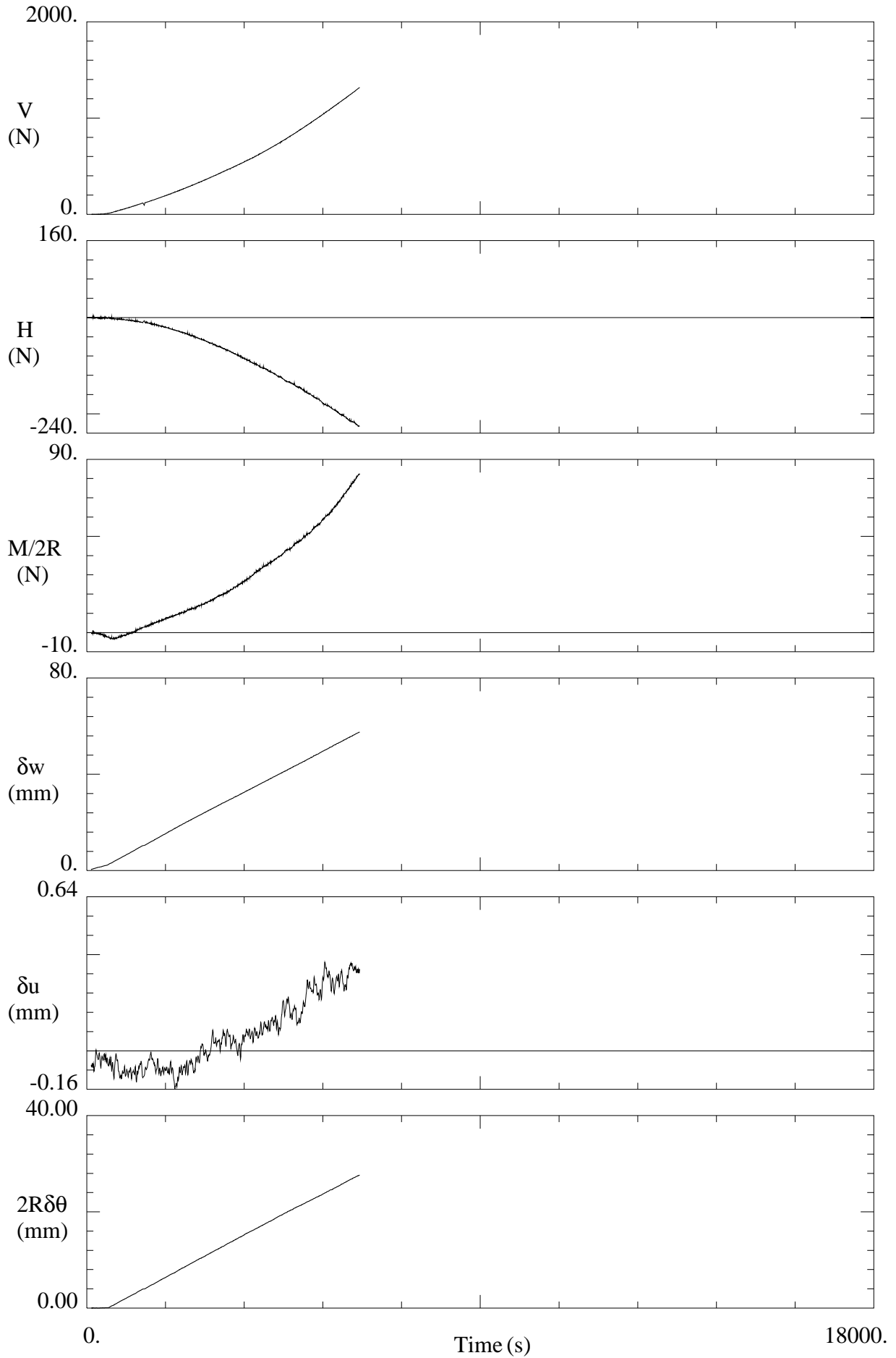


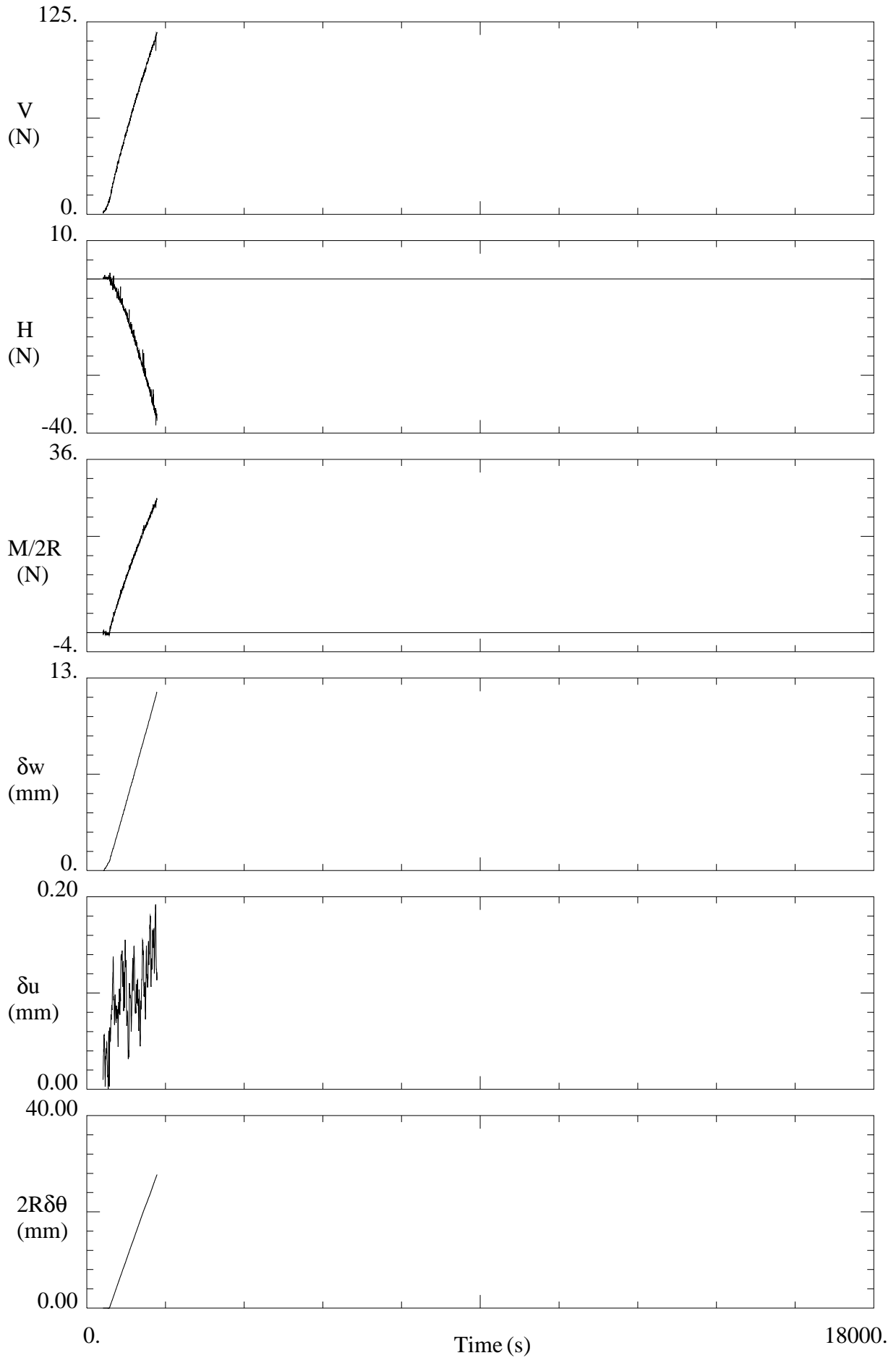
Oxford University: Carbonate Sand Footing Tests
Test FUF16: (H,-M) Swipe at Constant V=1600N











Oxford University: Carbonate Sand Footing Tests
Test FUF21: (H,0) Multiple Swipes from Various Loads

